Current **A**pplied **S**cience and **T**echnology e-ISSN: 2586-9396

Curr. Appl. Sci. Technol. ….., Vol... (No...), e0267980

Research article

Unraveling the Molecular Evolution and Structural Landscape of *Klebsiella pneumoniae* Carbapenemase Variants

Muhammad Yusuf Airlangga[1], Riffatih Syah Maharani[1], Amanda Rossiana Putri[1], Marita Tasya Andriasari[1], Balqis Salsabillah Shifa Fithryyah Cuhada[1], Nuraini Rosyadah[1], Fatchiyah Fatchiyah[1,2], Eko Suyanto[1,2] and Turhadi Turhadi[1]*

[1]Department of Biology, Faculty of Mathematics and Natural Sciences, Brawijaya University, Malang, East Java, Indonesia
[2]Research Center of Smart Molecule of Natural Genetics Resource, Brawijaya University, Malang, East Java, Indonesia

Received: 11 June 2025, Revised: 4 November 2025, Accepted: 2 December 2025, Published: 15 May 2026

Abstract

Mutations in the *bla*$_{KPC}$ gene significantly influence the effectiveness of antibiotics and combination therapies used to combat *Klebsiella pneumoniae* resistance. This study aimed to analyze genetic variations, physicochemical properties, and structural characteristics between mutant and wild-type class A β-lactamase KPC enzymes responsible for ceftazidime–avibactam resistance. Strains with the most significant mutations relative to the wild-type were identified based on physicochemical changes, haplotype networks, and structural conformations. The binding mechanisms between antibiotics and KPC enzymes were also evaluated to determine the role of conserved residues in enzymatic interactions and catalytic activity. Two wild types and 260 KPC variant sequences were retrieved from the NCBI database. ProtParam analysis indicated that all KPC variants exhibited stable physicochemical characteristics. Motif analysis using MEME revealed 15 conserved motifs across all variants. Phylogenetic tree reconstruction with MEGA 10 and iTOL, combined with haplotype analysis using DnaSP, identified KPC-2 and KPC-3 as ancestral variants. Protein modeling with AlphaFold and structural superimposition in PyMOL showed conformational shifts in the Ω-loop, 240-loop, and 270-loop regions. Molecular docking in PyRx demonstrated that ceftazidime acted as the strongest inhibitor against several KPC variants, which was supported by visualization using Discovery Studio 2025. Variants such as KPC-9, KPC-117, KPC-135, KPC-201, and KPC-258 showed the highest divergence, whereas those in Haplotype 1 remained closest to the wild-type. Mutations predominantly occurred within loop regions, while the protein core remained conserved, suggesting selective adaptation under antibiotic pressure. Further *in vitro* and *in vivo* validation is recommended to confirm in silico predictions and improve future therapeutic design.

Keywords: KPC (*Klebsiella pneumoniae* carbapenemase); mutant; haplotype; motif; phylogenetics

*Corresponding author: E-mail: turhadibiologi@ub.ac.id
https://doi.org/10.55003/cast.2026.267980

1. Introduction

Klebsiella pneumoniae is a Gram-negative bacterium that serves as a major cause of serious nosocomial infections such as pneumonia, urinary tract infection, and sepsis. Its pathogenic nature has drawn significant attention in terms of treatment, including antibiotic therapy (Ding et al., 2023). The emergence of multidrug-resistant strains in recent years has increased the prevalence of these infections. The Carbapenemase group exhibits resistance to antibiotics and is known as Carbapenemase-Resistant *Klebsiella pneumoniae* (CRKP), which has become a serious global medical concern. One of the main causes of this resistance is the presence of the *bla*$_{KPC}$ gene, which encodes a carbapenemase enzyme capable of hydrolyzing carbapenem antibiotics (Garsevanyan & Barlow, 2024). The increasing failure of β-lactam antibiotic therapies in *K. pneumoniae* infections across healthcare facilities has become a major issue, as it elevates the incidence of CRKP infections with high mortality rates (Sun et al., 2024).

The antibiotic combination ceftazidime-avibactam (CAZ-AVI) represents first-line therapy for CRKP infections. However, its clinical use has also led to reports of resistance, largely driven by mutations in the *bla*$_{KPC}$ gene (Wang et al., 2025). Ceftazidime (CAZ) belongs to the β-lactam antibiotic class and is often considered a “last-resort” therapy for resistant bacterial infections, making resistance to it particularly concerning (Bongiorno et al., 2023). These mutations generally occur in functional regions of the gene that alters enzyme affinity toward avibactam (AVI) and increase hydrolytic activity against CAZ, thereby reducing inhibitor efficacy (Hobson et al., 2022). *bla*$_{KPC}$ mutations may involve point substitutions, insertions, or deletions, which not only lead to treatment failure but also complicate laboratory detection, as some variants cannot be identified by conventional phenotypic methods (Sun et al., 2021; Zhang et al., 2024). The limited therapeutic options and reduced antibiotic efficacy due to emerging *Klebsiella pneumoniae* carbapenemase (KPC) mutant variants are expected to worsen the clinical burden and promote interbacterial resistance spread via plasmids (Qiao et al., 2024).

In clinical isolates, several *bla*$_{KPC}$ mutant variants have been identified that confer resistance to CAZ. Some mutations even lead to reduced resistance to carbapenems, shifting from highly resistant to more susceptible as an adaptive mechanism to evade AVI. Mutations that increase resistance to CAZ often result in decreased resistance to other antibiotics (a trade-off effect) (Shields et al., 2017; Ding et al., 2023). Globally, numerous infection cases have been reported involving KPC mutant variants encoding resistance to CAZ. Based on these findings, it is predicted that KPC enzymes have evolutionary potential to develop mutations conferring resistance to β-lactam/β-lactamase inhibitor combination therapies (Shi et al., 2022). Since the clinical introduction of CAZ for *K. pneumoniae* infections, more than 260 KPC mutant variants have been identified, predominantly in strains from the United States, China, Italy, and other European countries, and their number continues to rise exponentially (Giddins et al., 2018).

Resistance to CAZ is primarily caused by conformational alterations in the Ω-loop and the active site of enzyme that enhance hydrolytic activity toward ceftazidime while reducing affinity for AVI. Reports of infections caused by KPC mutant variants signal that resistance evolution is ongoing. This situation is concerning, especially in regions with high population density and mobility, as it increases the risk of cross-border spread and horizontal transfer through plasmids within hospital environments (Zhang et al., 2024, 2025). Besides imipenem (IPM) and meropenem (MEM), other β-lactam antibiotics such as aztreonam (ATM), and the combination of CAZ-AVI are also used for treating *K. pneumoniae* infections. ATM is relatively stable against most β-lactamases but can still be

hydrolyzed by KPC, and especially by mutants with alterations in the active site. IPM and MEM are often used as benchmarks to assess the catalytic activity of class A β-lactamases due to their distinct interactions with active-site residues (Satapoomin et al., 2022).

Horizontal Gene Transfer (HGT) plays a key role in accelerating the emergence and spread of KPC mutant variants. The *bla*$_{KPC}$ gene can be transferred horizontally between bacteria, including across species and genera, allowing direct plasmid-mediated genetic exchange even among unrelated organisms (Partridge et al., 2018). This horizontal transfer does not occur through vertical inheritance from parent to offspring but through conjugation, transformation, and transduction. Furthermore, the presence of mobile genetic elements commonly associated with *bla*$_{KPC}$ enhances its ability to integrate into various genomes and spread widely (Acman et al., 2022). This study employs wild-type KPC-2 and KPC-3 as main references since they represent the earliest and most clinically prevalent variants, considered ancestral types for hundreds of emerging KPC mutants. KPC-2 is structurally stable, whereas KPC-3 exhibits enhanced hydrolytic activity toward certain β-lactams (Huang et al., 2023; Falagas et al., 2025).

The global antibiotic resistance crisis and the therapeutic limitations of CAZ against *K. pneumoniae* strains constitute major health concern. Analyzing 260 KPC mutant sequences alongside two wild-type sequences (KPC-2 and KPC-3) is crucial to gain insights into mutation patterns and their distribution (Fontana et al., 2021; Sanz et al., 2024). Understanding KPC mutations and their impact on antibiotic resistance will aid in determining effective antibiotic combinations and developing new therapeutic strategies and infection-control policies. Therefore, this study aims to analyze the structural and functional differences between mutant and wild-type class A β-lactamase KPC enzymes responsible for resistance to CAZ-AVI in *K. pneumoniae*. It also seeks to examine the genetic variation between mutant and wild-type strains and identify variants with the most significant or wild-type-like mutations based on physicochemical properties, haplotype networks, and conformational changes.

2. Materials and Methods

2.1 Sequence data mining

The *bla*$_{KPC}$ nucleotide and KPC amino acid sequences consisting of two wild-types and all mutant variants with annotated function as KPC up until 10th May 2025 were collected from the National Center for Biotechnology Information (NCBI) database (http://www.ncbi.nlm.nih.gov/) with a total of 260 mutant variants. Wild-type and mutant variants sequences from NCBI were saved in FASTA format. Then, sequences were submitted to numerous web server tools for further analysis.

2.2 Physicochemical properties analysis

Physicochemical properties were analyzed in ExPAsy ProtParam (https://web.expasy.org/protparam/) by submitting FASTA format of KPC wild-type and mutant sequences. ExPASy ProtParam was used for protein physicochemical characterization based on certain parameters, such as molecular weight, isoelectric point, aliphatic index, instability index, amino acid composition, and grand average of hydropathy (GRAVY). This analysis was performed to compare protein physicochemical properties between each variant of KPC sequences (Rubalakshmi et al., 2020).

2.3 Sequences motifs analysis

Amino acid sequences of KPC wild-type and mutant variants were analyzed using Multiple Em for Motif Elicitation (MEME) ver 5.5.7 (https://meme-suite.org/). A data submission form was filled in first, this included configuring the parameters for the motif distribution and typing in the protein sequence as the input. The other MEME default configurations were maintained. Motifs analysis provided information about the conserved region found in every protein sequence, indicating potential important structure (Bailey et al., 2015).

2.4 Phylogenetic tree and haplotype construction analysis

Nucleotide sequences of KPC variants were used to construct a phylogenetic tree and CTX-M-1 as the outgroup of the tree (Garsevanyan & Barlow, 2024). The phylogenetic tree was constructed using the Kimura 2-parameter model (K2) with Gamma Distributed with Invariant Sites (G+I) algorithm, Poisson substitution model with the bootstrap number of 1000, in Molecular Evolutionary Genetics Analysis (MEGA) version X (Rocha et al., 2022). Then, the phylogenetic tree construction result was edited in Interactive Tree of Life (iTOL) (https://itol.embl.de/) for better visualization. The nucleotide sequences of *bla*$_{KPC}$ variants, except for KPC-41 (MK497255.1) due to the ambiguous sequence, were used as the input in DnaSP6 v6.12.03 to generate the haplotype input dataset. Next, the haplotype network was drawn from the generated haplotype dataset in Network 10.2.0.0 software. The haplotype network was performed to determine mutation distance between *bla*$_{KPC}$ variants (Rozas et al., 2017).

2.5 Protein visualization

The three-dimensional structures of the wild-type and mutant KPC proteins were predicted in AlphaFold web server (https://alphafold.ebi.ac.uk/). Modeling was performed based on the amino acid sequences of both the wild-type and mutant forms. The resulting 3D structural models were selected based on sequence identity. Model assessment was further conducted using TED domains and Predicted Aligned Error (PAE) (Lau et al., 2024). Then, the 3D structure alignment was performed using PyMOL Molecular Graphics System, version 3.1.3.1 (Schrödinger, LLC.) to observe any conformational changes in protein and the aligned structure between the wild-type and mutant variants.

2.6 Molecular docking

Ligands in the form of antibiotics were prepared using PyRx Ver 0.8 software. Ligand preparation was carried out using the Open Babel feature in PyRx to minimize the energy of each ligand. Ligands whose energy had been minimized were converted into PDB format (Wargasetia et al., 2021; Widyananda et al., 2023). Meanwhile, the preparation of the KPC variant receptor was carried out by removing water molecules and ligands integrated in its three-dimensional structure (Permana et al., 2024). The software used was BIOVIA Discovery Studio Visualizer Ver 25.1.0.24284 and PyMOL 3.1.3.1. The prepared KPC variant ligands and proteins were then docked with maximum grid and the exhaustiveness were set at 50 using Vina Wizard integrated in PyRx Ver 0.8 (Rachmi et al., 2020).

3. Results and Discussion

3.1 KPC variants physicochemical properties analysis

Physicochemical properties analysis was computed in Expasy ProtParam web with certain parameters to predict the stability from 2 wild-type and 260 mutant variants of amino acid KPC. The physicochemical properties of KPC variants were analyzed based on several parameters: number of amino acids, molecular weight, isoelectric point (pI), instability index, aliphatic index, and the grand average of hydropathy (GRAVY). Based on Table 1, variants of KPC sequences had numbers of amino acids ranging between 290-308 with molecular weights ranging between 29599.67-34081.74 Da. From Figure 1, each variant of amino acid KPC had isoelectric point (PI) values from 5.96-8.92, instability index ranging between 26.91-32.74, aliphatic index values ranging between 86.24 - 91.12, and grand average of hydropathy (GRAVY) values ranging between -0.113 to 0.The overall values of the physicochemical analysis showed that variants of KPC had good quality and stability.

The physicochemical properties of a protein consist of several parameters including number of amino acids, molecular weight, isoelectric point (pI), instability index, aliphatic index, and the grand average of hydropathy (GRAVY). Amino acids are the building blocks of proteins and serve crucial functions as structural elements and energy sources for normal cell growth and metabolism (Ling et al., 2023). Molecular weight can affect the physical and chemical properties of a protein, affecting the behavior and cellular function of protein (Mohanta et al., 2022). The isoelectric point (pI) is a parameter that indicates the pH of protein. If the value is less than 7, the protein has acidic character and if the isoelectric point value is more than 7, the protein has alkaline character (Rubalakshmi et al., 2020). The instability index is a parameter that indicates protein stability. If the value is less than 40, it is predicted to be a stable protein and the protein is predicted to be unstable if the value is more than 40 (Guruprasad, 2016). Aliphatic point indicating the aliphatic site of protein structure, if the value is closer to 100 meaning the protein has good structure quality (Gouripur et al., 2016). If the grand average of hydropathy (GRAVY) value is closer to negative, it indicates that the protein is hydrophilic and the value near to positive indicates the protein is hydrophobic (Rubalakshmi et al., 2020). Therefore, physicochemical variants of KPC varied in isoelectric point (pI), aliphatic index, and GRAVY, indicating that these parameters may be the key patterns and causes of mutant variants in KPC.

Table 1. Number of amino acid and molecular weight of class-a β-lactamase kpc variants

Protein	Number of Amino Acid	Molecular Weight (Da)
KPC-2 (Wild-type)	293	31115.35
KPC-3 (Wild-type)	293	31141.39
KPC-4 – KPC-272 (260 variants)	290-308	29599.67 - 34081.74

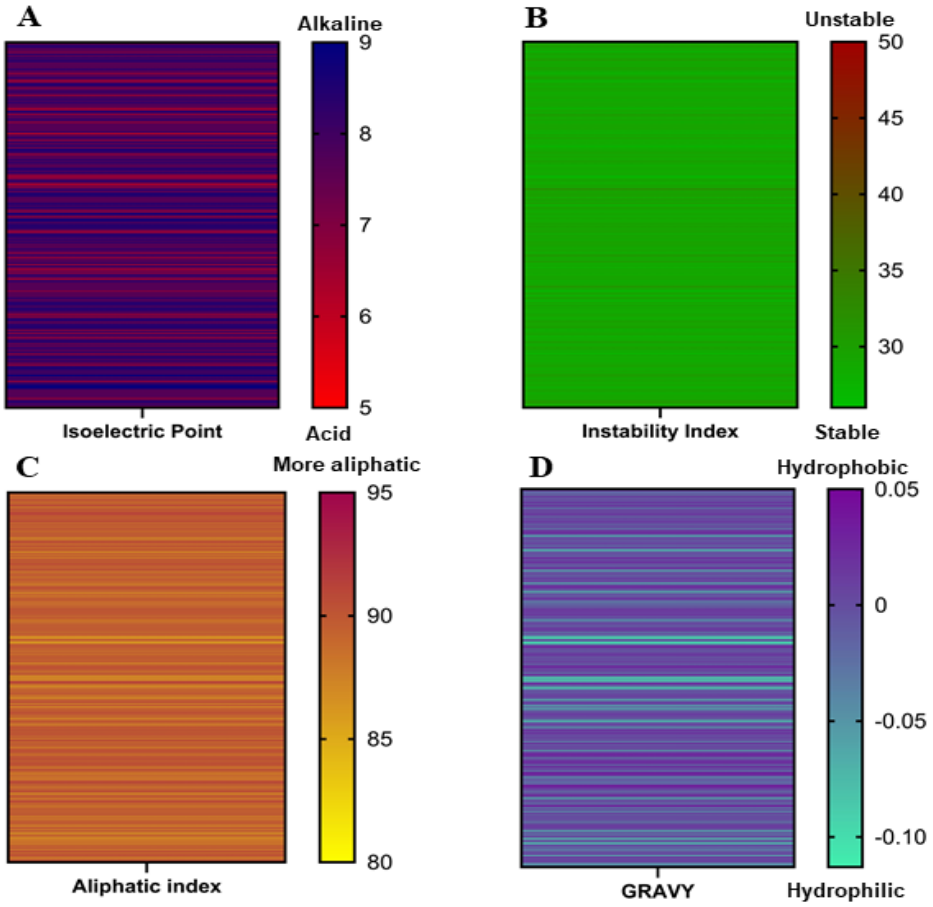

Figure 1. Physicochemical analysis of class-A β-lactamase KPC variants. (A) Isoelectric point. (B) Instability index. (C) Aliphatic index. (D) Grand average of hydropathy (GRAVY)

3.2 KPC variants haplotype and phylogenetic tree construction analysis

Haplotype network construction was performed to visualize the relationship between different haplotypes of KPC variants from the DNA sequences. The haplotype network in Figure 2 illustrates the mutation distance between 49 haplotypes, and each haplotype consists of a single, or multiple KPC variants. Haplotype 1 (Hap_1) is the most commonly found haplotype and is drawn as the center of the network, which includes the wild-type that are KPC-2 and KPC-3, and hundreds of other KPC variants (Table 2). Haplotype 1 can be considered as the ancestral haplotype of others, and the size of Haplotype 1 is larger than other haplotypes, indicating high frequency and genetic dominance. This reflects variants that are very similar to each other, although there is a possible slight difference in the nucleotide sequence. The red numbers on the branches of the haplotype network represent the position of the mutation or single-nucleotide change in the DNA sequence alignment that distinguishes the connected haplotypes.

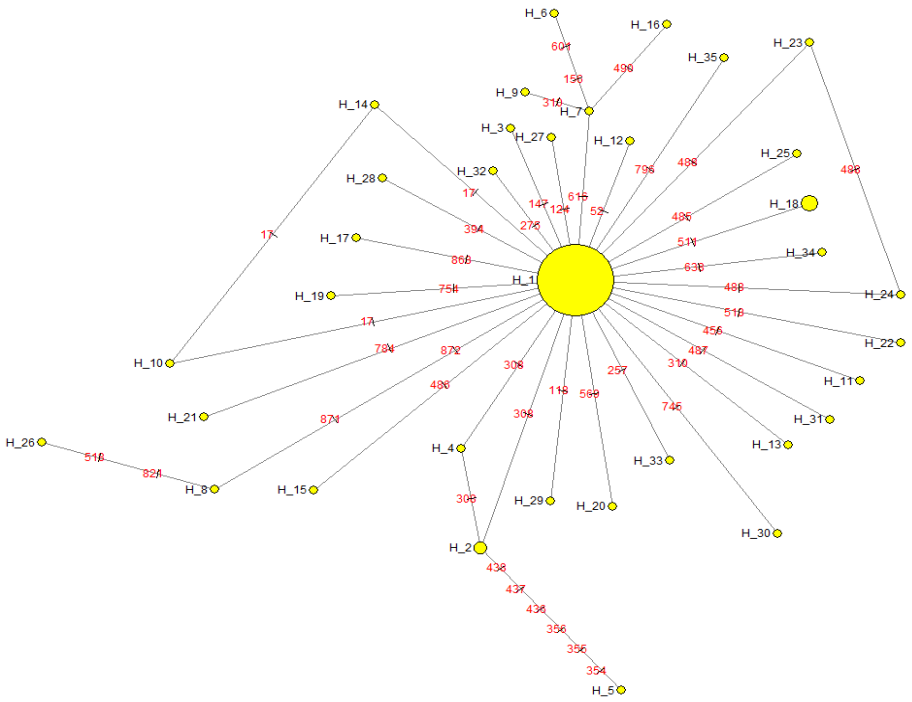

Figure 2. Haplotype analysis of class-A β-lactamase KPC variants

Table 2. Haplotype network data input of class-a β-lactamase kpc variants

Haplotype	KPC Variants
Hap_1	KPC-2 KPC-3 KPC-6 KPC-8 KPC-9 KPC-12 KPC-14 KPC-19 KPC-23 KPC-28 KPC-29 KPC-31 KPC-32 KPC-33 KPC-34 KPC-35 KPC-36 KPC-38 KPC-39 KPC-40 KPC-44 KPC-46 KPC-47 KPC-48 KPC-49 KPC-50 KPC-51 KPC-52 KPC-53 KPC-56 KPC-57 KPC-58 KPC-61 KPC-62 KPC-63 KPC-65 KPC-66 KPC-67 KPC-68 KPC-69 KPC-71 KPC-72 KPC-73 KPC-74 KPC-76 KPC-77 KPC-78 KPC-79 KPC-80 KPC-81 KPC-82 KPC-84 KPC-85 KPC-86 KPC-87 KPC-88 KPC-89 KPC-90 KPC-92 KPC-93 KPC-94 KPC-95 KPC-96 KPC-97 KPC-98 KPC-99 KPC-100 KPC-101 KPC-102 KPC-103 KPC-104 KPC-105 KPC-106 KPC-107 KPC-108 KPC-109 KPC-111 KPC-112 KPC-113 KPC-114 KPC-115 KPC-116 KPC-121 KPC-123 KPC-124 KPC-125 KPC-126 KPC-127 KPC-128 KPC-129 KPC-130 KPC-132 KPC-133 KPC-134 KPC-135 KPC-136 KPC-137 KPC-138 KPC-139 KPC-140 KPC-141 KPC-142 KPC-144 KPC-146 KPC-148 KPC-150 KPC-151 KPC-152 KPC-153 KPC-154 KPC-155 KPC-159 KPC-160 KPC-161 KPC-162 KPC-163 KPC-164 KPC-165 KPC-166 KPC-167 KPC-168 KPC-169 KPC-170 KPC-171 KPC-172 KPC-173 KPC-174 KPC-175 KPC-176 KPC-177 KPC-178 KPC-180 KPC-181 KPC-183 KPC-184 KPC-185 KPC-186 KPC-187 KPC-188 KPC-189 KPC-191 KPC-192 KPC-193 KPC-196 KPC-197 KPC-201 KPC-202 KPC-203 KPC-204 KPC-205 KPC-206 KPC-207 KPC-208 KPC-209 KPC-211 KPC-212 KPC-213 KPC-214 KPC-215 KPC-216 KPC-217 KPC-218 KPC-220 KPC-224 KPC-225 KPC-226 KPC-227 KPC-228 KPC-230 KPC-231 KPC-233 KPC-234 KPC-237 KPC-238 KPC-239 KPC-240 KPC-241 KPC-242 KPC-243 KPC-245 KPC-250 KPC-251 KPC-252 KPC-255 KPC-256 KPC-257 KPC-258 KPC-259 KPC-260 KPC-261 KPC-262 KPC-263 KPC-265 KPC-266 KPC-267 KPC-268 KPC-269 KPC-270 KPC-271 KPC-272

Phylogenetic tree reconstruction was performed to observe the evolutionary distance and relationship between 260 mutant strain sequences compared to the wild-type variants. Figure 3 shows the results of phylogenetic tree reconstruction. Each phylogenetic branch shows one KPC variant with several main branches indicating a large evolutionary distance between groups.

KPC-2 is the earliest KPC variant and the ancestor of other KPC variants, while KPC-3 is the earliest mutant of KPC-2. The existence of KPC-2 and KPC-3 in Haplotype 1 emphasizes that Haplotype 1 is the ancestral haplotype. Meanwhile, other haplotypes are considered to be the result of mutations derived from Haplotype 1, either directly or indirectly. This is also in line with the fact that KPC-2 is considered an early variant of KPC and is the basis for the emergence of various other KPC variants. Meanwhile, KPC-3 emerged as a result of a mutation in KPC-2, so it is considered one of the early variants that came directly from KPC-2 (Hobson et al., 2022). Most of the newly emerged KPC variants come directly or indirectly from KPC-2 and KPC-3, each through a single mutation (Tsai et al., 2021; Wei et al., 2025).

The presence of the HGT phenomenon caused by local spread makes KPC mutations easy to occur. Based on all the KPC variants found, most of the new variants came from KPC-2 and KPC-3, which was around 91%. This was due to the acceleration of evolution and diversification of variants as a result of the selection pressure of new antibiotics such as ceftazidime-avibactam. These variants carry one major amino acid change that can affect the resistance profile to antibiotics (Wang et al., 2014; Chen et al., 2022). The KPC mutation that appeared earlier was KPC-2 and was followed by KPC-3, which is the reason why the derivative mutation variants were found more than the KPC-3 derivatives. The difference between KPC-2 and KPC-3 lies in sequence 272, where a substitution underwent from the amino acid residue H or histidine to T or tyrosine (H272Y) (Migliorini et al., 2021).

The *bla*$_{KPC}$ gene is located on a conjugative plasmid that can transfer between bacteria, where this plasmid is independently conjugative because it has a transfer gene that enables direct transfer to other cells through the process of conjugation. KPC on the KPC-2 plasmid has spread widely to various bacterial species through plasmids carrying the Tn4401 transposon. In addition, the plasmid that spreads blaKPC plays an important role in enabling the accumulation of mutations at structural hotspots, especially in several loops that alter the three-dimensional conformation around the conserved motif. These changes cause plasmids carrying KPC variants with more stable and efficient active motifs to have a greater chance of being selected evolutionarily and spreading globally, accelerating the process of antibiotic resistance spread in various environments (Hobson et al., 2022; Xie et al., 2025).

Plasmid-mediated conjugation is the primary mechanism driving the rapid horizontal spread of the bla$_{KPC}$ gene in *K. pneumoniae*. In most cases, bla$_{KPC}$ is found on self-transferable plasmids, often from the IncN or IncF incompatibility groups, which enable transfer between bacteria (both intra- and interspecies) via the conjugation machinery encoded in these plasmids. For example, plasmids carrying *bla*$_{KPC-2}$ on the IncN or IncFII framework were shown to transfer efficiently via conjugation (Rada et al., 2020). In addition, another mechanism of spread may involve *bla*$_{KPC}$ being mobilized into plasmids, transposable elements such as Tn4401, which plays an important role by inserting genes into the plasmid backbone, thereby enabling the transfer of *bla*$_{KPC}$ between plasmids or from one plasmid to another within the same cell (Sugita et al., 2021).

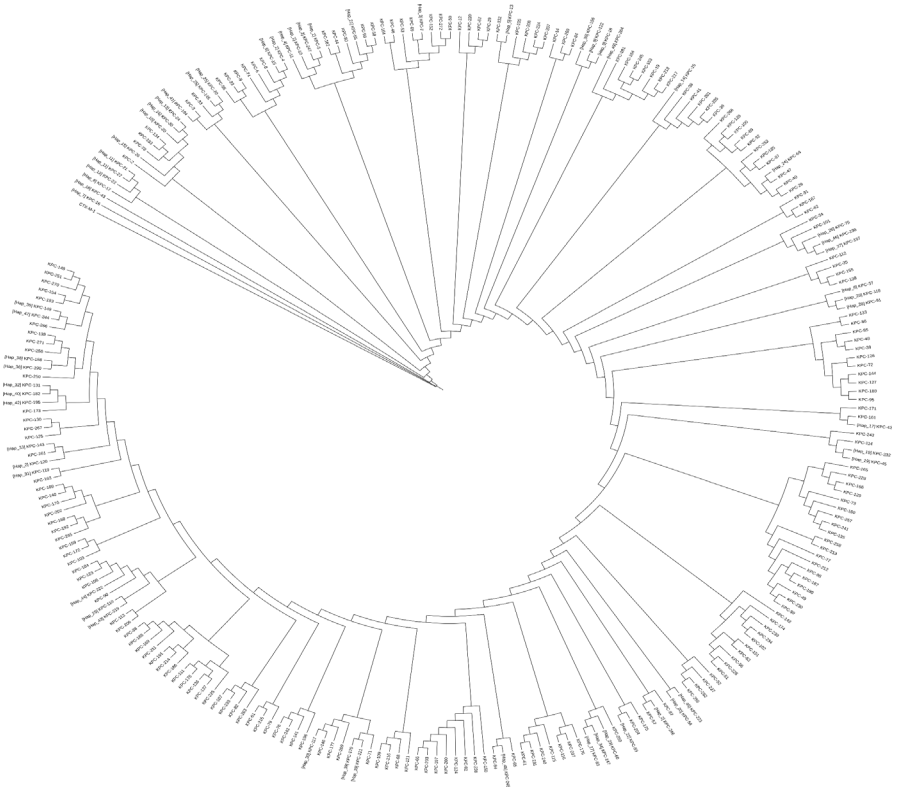

Figure 3. Class -A β-lactamase KPC variants phylogenetic tree

In addition to the Tn4401 system, non-Tn4401 elements which are collectively referred to as NTE_KPC and insertion sequences, particularly IS26, facilitate the reorganization of the genetic context surrounding bla_{KPC}. IS26 can mediate homologous recombination, plasmid cointegration, deletion, or duplication, resulting in new plasmids containing bla_{KPC} or altering the expression level of this gene. Additionally, the formation of promiscuous plasmids occurs through plasmid cointegration and recombination, which involve plasmids fusing, exchanging segments, or acquiring replicon frameworks with a broader host range due to events mediated by IS or transposons (Guo et al., 2022). Furthermore, another mechanism of spread occurs when plasmids containing bla_{KPC} enter *K. pneumoniae* clones, where clonal expansion plays a role in strengthening and stabilizing the presence of the gene. Thus, horizontal transfer establishes new hosts, and clonal spread forms a stable reservoir (Brandt et al., 2019).

The global spread of the KPC gene has led to a significant increase in antibiotic resistance in various countries. This phenomenon can occur due to two main factors, namely clonal development through strain spread and horizontal gene transfer, which allows the transfer of genes between bacterial species. Bacterial strains that are dominant in a region usually carry plasmids with beneficial adaptive effects, causing variations in plasmid profiles between regions and over time. Local outbreaks of the same strain can reinforce the dominance of these plasmids, supporting the continued spread of resistance genes. Although most KPC plasmids circulate only within *K. pneumoniae* groups, the ability of plasmids to transfer to other bacterial species plays an important role in interspecies

spread. Therefore, research on the dynamics of these plasmid movements in various environments is crucial for understanding how KPC genes evolve, adapt, and spread (Cai et al., 2024).

3.3 KPC variant protein motifs analysis

Protein sequence motif analysis of 2 wild-type and 260 KPC mutant variants was performed in MEME. Based on Figure 4, fifteen conserved motifs of class-A β-lactamase KPC and its mutations were discovered. Motif 14 shows higher variability in the amino acid sequence compared to other motifs (Figure 4). Fifteen motif locations are distributed in all sequences at nearly the same locations. Motif 1 is located around amino acid numbers 201-238, identified as the K-T-G motif and its surrounding structural elements. Motif 2 is located around amino acid numbers 25-74, covering the catalytic serine (S70) and the S-X-X-K motif around amino acid numbers 70-73. Motif 3 is located around amino acid number 82-131, covering the SDN (Ser-Asp-Asn) loop structure. Motif 4 is located around amino acid numbers 134-160, positioned immediately after the SDN loop. Motif 5 is located around amino acid numbers 244-264; this motif is situated within the region encompassing portions of the 240-loop and preceding the 270-loop. The broad conservation of this motif implies its importance for structural integrity around this area. Motif 6 is located around amino acid numbers 277-293, identified as the C-terminus of the enzyme. Motif 7 is located around amino acid numbers 182-197; this motif is located immediately downstream of the omega loop structure. Its positional variability suggests it might act as a flexible linker region, connecting the dynamic omega loop to other more stable parts of the protein, or influencing the omega loop's conformation. Motif 8 is located around amino acid numbers 7-21, identified as the N-terminus of the enzyme.

Motif 9 is located around amino acid numbers 244-264; this motif is a sub-region within the broader segment covered by Motif 5. Motif 10 is located around amino acid numbers 169-181, covering the Ω-loop structure. Motif 11 is located around amino acid numbers 161-168, this motif located upstream of the Ω-loop structure. Motif 12 is located around amino acid numbers 1-6, identified as part of the N-terminus of the enzyme. Motif 13 is located around amino acid numbers 75-80; this motif is located close to the serine catalytic residue. Motif 14 is located around amino acid numbers 169-179 and only exists in some KPC variants. This motif has the same sequence as the Ω-loop structure, indicating there is Ω-loop duplication. Motif 15 is located around amino acid numbers 265-270 and only exists in some KPC variants. It is always placed immediately downstream of motif 5.

Based on Figure 5, KPC-44 motif composition exhibits omega-loop amino acid duplication before the C-terminus, and this motif composition could be found in other KPC variants such as KPC-103, KPC-105, and KPC-148. The KPC-66 motif composition exhibits omega-loop amino acid duplication, and this motif composition could be found in other KPC variants such as KPC-92, KPC-94, KPC-112, KPC-115, KPC-124, KPC-160, KPC-166, KPC-197, KPC-203, KPC-216, KPC-237, KPC-238, and KPC-260. The KPC-58 motif composition exhibits motif 15 insertion, and this motif composition could be found in the other KPC variants such as KPC-67, KPC-109, KPC-129, KPC-132, KPC-134, KPC-139, KPC-162, KPC-163, KPC-183, KPC-220, KPC-230, KPC-245, KPC-261, and KPC-271. The KPC-257 exhibits motif 15 addition with different omega loop motifs, and this motif composition could be found in the KPC-73. The KPC-81 motif composition exhibits undiscovered motif in the omega-loop core area, and this motif composition could be found in the other KPC variants such as KPC-169, KPC-186, KPC-191, KPC-211, KPC-225,

KPC-228, KPC-240, and KPC-241. The KPC-133 motif composition exhibits omega-loop amino acid duplication between motif 9 and motif 5, before the C-terminus, and this motif composition could be found in the other KPC variants such as KPC-108, KPC-140, KPC-152, KPC-154, KPC-192, KPC-251, KPC-256, KPC-265, and KPC-270. KPC-135 suggests an undiscovered omega-loop core motif and omega-loop amino acid duplication between motif 9 and 5, before the C-terminus, and this motif composition can only be found in KPC-135. The KPC-258 motif composition suggests undiscovered whole omega-loop motif, and this motif composition can only be found in KPC-258. The KPC-201 motif composition suggests a chance of an undiscovered pre-omega-loop motif, and this motif composition can only be found in KPC-201. The KPC-117 motif composition exhibits undiscovered N-terminus, and this motif composition can only be found in KPC-117. The KPC-9 motif composition exhibits undiscovered motifs at the N-terminus and C-terminus region, and this motif composition can only be found in KPC-9.

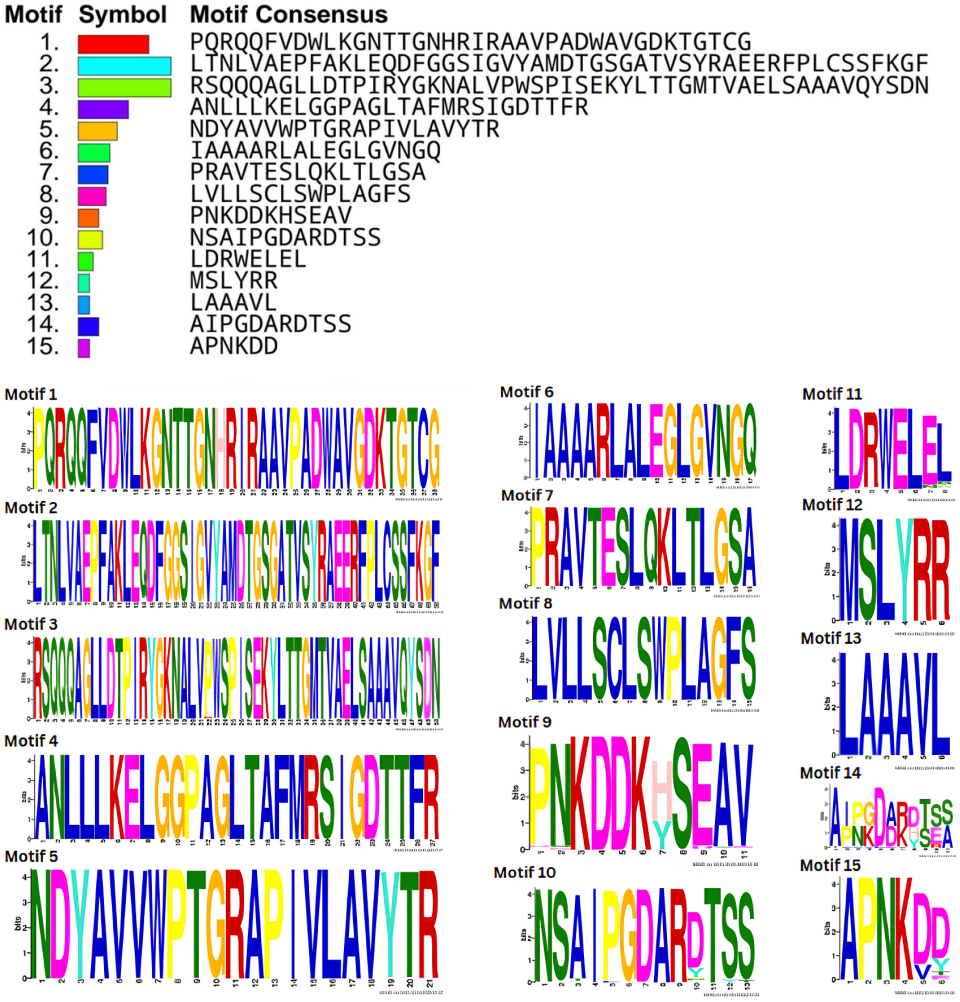

Figure 4. Class-A β-lactamase KPC variant protein motif analysis

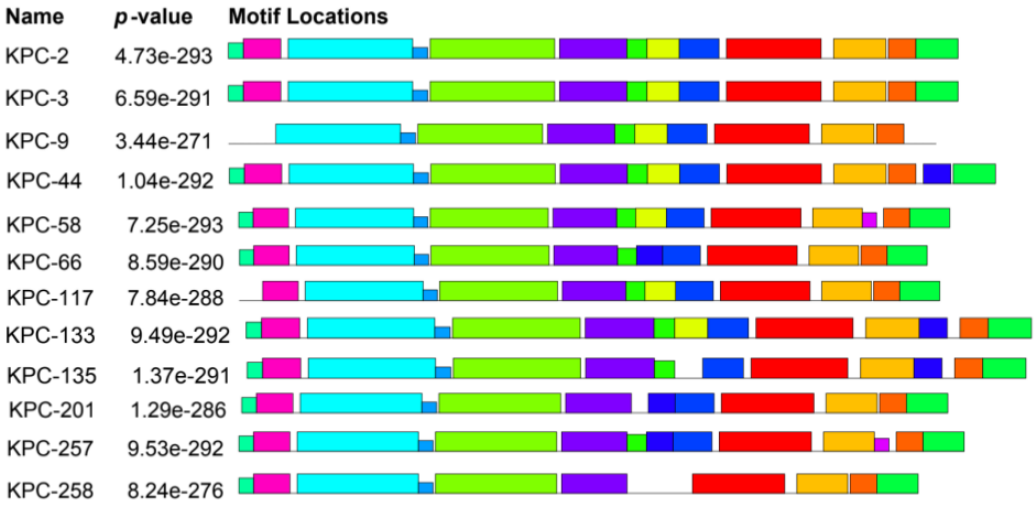

Figure 5. Several class-A β-lactamase KPC variants motif comparison

The catalytic serine residue (Ser70), as covered in motif 2, plays a central and crucial role in the hydrolysis and inactivation of beta-lactam antibiotics, especially in acylation and deacylation catalytic mechanisms. The catalytic Ser70 residue hydroxyl group acts as a powerful nucleophile, launching a nucleophilic attack on the carbonyl carbon of the four-membered beta-lactam ring in the antibiotic molecule, leading to the cleavage of the amide bond within the beta-lactam ring. Simultaneously, a covalent acyl-enzyme intermediate is formed, where the antibiotic is temporarily bound to Ser70. Following the acylation, a catalytic water molecule enters the active site and attacks the carbonyl carbon of the acyl- enzyme intermediate. This attack hydrolyzes the ester bond between Ser70 and the now-inactivated drug resulting in release of the hydrolyzed antibiotic product, regenerating the free catalytic Ser70, and allowing the enzyme to catalyze another reaction cycle (Hobson et al., 2022; Sun et al., 2024; Tooke et al., 2023).

The SDN motif as covered in motif 3, plays a role in forming a cationic patch that directly interacts with the carboxamide carbonyl oxygens of the beta-lactam antibiotic core structure for proper substrate binding and efficient catalytic function. When mutations occur within this motif, such as N132G, it can significantly disrupt enzyme ability to bind substrates or alter its interaction with beta-lactamase inhibitors like AVI and clavulanate (Ourghanlian et al., 2017). There are three loop structures found in KPC that possess important functions in enzyme activity and resistance evolution, specifically Ω-loop, 240-loop, and 270-loop. These 3 loops form the enzyme catalytic pocket. The conformation and flexibility of this pocket influence the substrate or antibiotics specificity binding and hydrolysis efficiency. Any mutations in these loop regions are common mechanisms by which KPC variants acquire resistance to the existing or new beta-lactam antibiotics and beta-lactamase inhibitors (Wei et al., 2025).

Motifs that have a high level of conservation are often found in closely related variants, indicating that the variants originated from the same ancestor. However, the emergence of different and less conservative motifs indicates evolutionary divergence when the species has adapted to its surroundings. The differences in motifs among the

entire class-A β-lactamase KPC variant sequences are also caused by molecular mechanisms in the form of deletions in which part of the motif is lost, addition in the form of insertions of new sequences in the motif, and mutations that result in small differences in the motif. This shows a high level of conservation between variants, which suggests that these amino acid sequences may play a role in the same molecular function (Moraes Filho et al., 2017).

3.4 KPC variants 3D structure comparison

Eleven KPC variants were chosen based on the motif composition difference (Figure 5), then three-dimensional (3D) structure modeling and structural superimposition analyses were conducted to further understand how these motif variations affected the structural and functional properties of KPC variants. The superimposition of the 3D structures generated from the modeling of wild-type and mutant KPC variants seen in Figure 6 predominantly revealed conformational changes in the loop regions. In contrast, the core structures remained conserved, with no notable conformational alterations detected. In the visualizations, the wild-type structure is represented in red, the mutant variants in blue, and the regions undergoing conformational change were highlighted in green within the 3D structure model. Based on the visualization results obtained, the conformational changes that occurred were of different types, namely hinge motion, rearrangement, and fold switch. The hinge motion conformational change was produced by KPC-117 and KPC-9. The rearrangement type was produced by the motif composition found in KPC-44, KPC-66, KPC-58, KPC-257, KPC-133, KPC-135, KPC–258, and KPC-201. Meanwhile, the fold switch conformational change was produced by KPC-81. Changes in protein structure conformation have the potential to disrupt its interaction with the β-lactam substrate so that increased resistance of a bacterium to β-lactam antibiotics might increase.

Protein conformational changes can occur due to received signals, such as chemical modifications, ligand binding, and environmental changes. Protein structural changes can also be stimulated by phosphorylation, which includes covalent modifications. The resulting protein structural conformational changes can modulate enzymatic activity or even show new surfaces for proteins so that they can interact with other molecules (Ha & Loh, 2012). According to Bryant and Noé (2024), conformational changes in proteins did not all follow the same type; some involve fold changes, while others only involve movement of one domain near the hinge. Hinge motion is a conformational change in which most of the structural domains remained the same, while the relative orientation between the domains changed. Rearrangement is a type of conformational change in protein structure where the tertiary structure of the domain changed, but the secondary structure remained mostly the same. Fold switch refers to a change from an alpha helix to a beta loop or beta sheet, and vice versa. Thus, the evolution of KPC is largely influenced by the functional properties of the active loop without requiring a change in the entire protein framework.

KPC-44 exhibits conformational change in the 3D structure because of 15 amino acids duplication (Ala262-Glu276) at 270-loop. This insertion leads to significant conformational changes in the 270-loop and adjacent 240-loop, which critically reduces the efficiency of AVI inhibition and increases the catalytic efficiency for CAZ, but with a potential trade-off in carbapenem hydrolysis efficiency (Sun et al., 2024). KPC-115 possesses CAZ-AVI resistance attributable to two-point deletions at sequence 167 and 168, and two mutations in the X-loop (a region encompassing or near the Ω-loop). Similarly to KPC-44, KPC-115 also shows resistance to CAZ-AVI accompanied by a trade-off in carbapenem

susceptibility, even though the molecular mechanisms underlying this phenomenon are different (Nicola et al., 2022). KPC-109 is characterized by a six-amino acid insertion (KYNKDD) in its 270-loop. This insertion is analogous to the 15 amino acids and duplication seen in KPC-44, although it is a different specific insertion and arises from KPC-3 as the wild-type. KPC-109 conformational change enables this variant to resist CAZ and cefiderocol. While it can show a trade-off resulting in carbapenem susceptibility, this can be masked or overcome in clinical settings by co-occurring resistance mechanisms like porin deficiencies (Pilato et al., 2024).

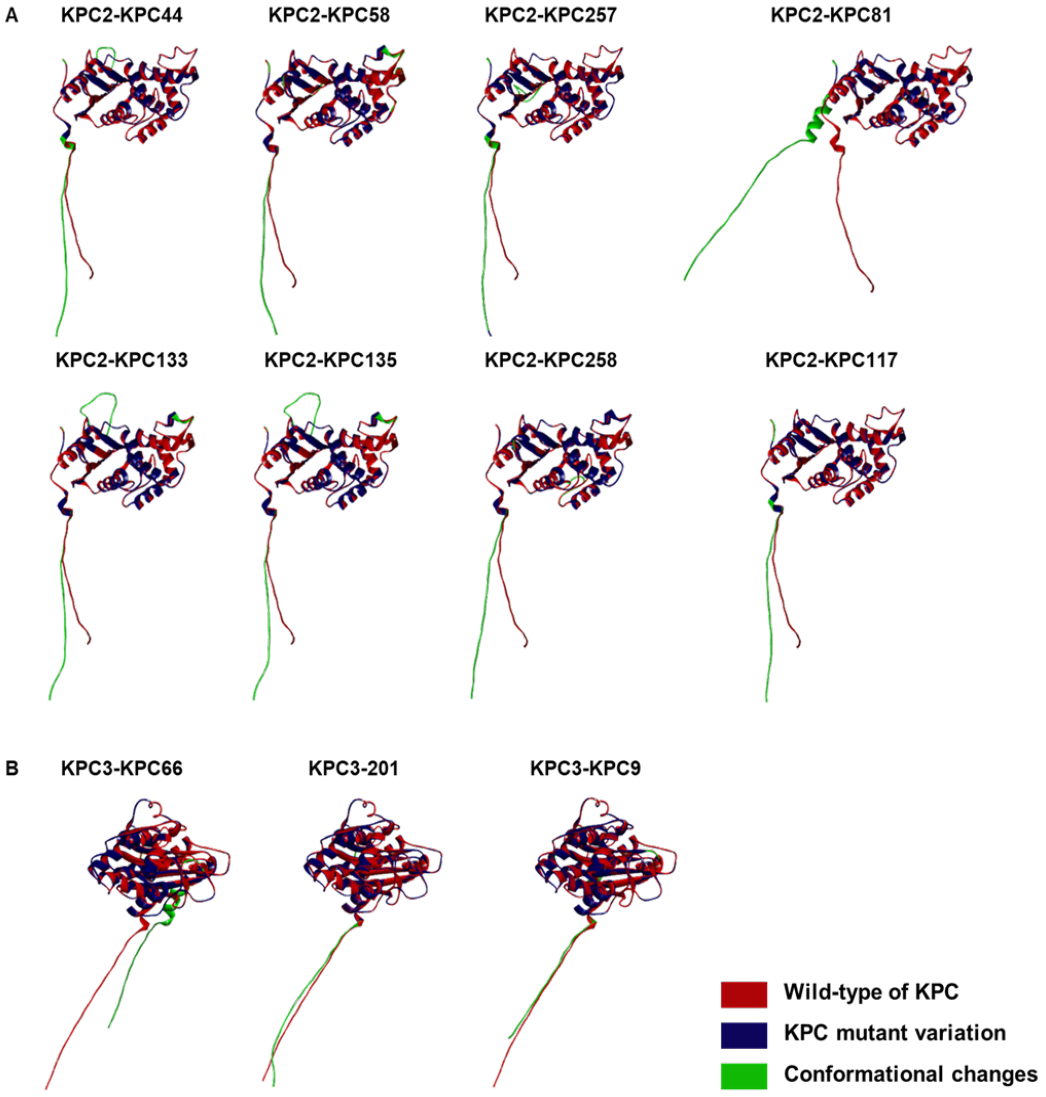

Figure 6. Class A β-lactamase KPC variants 3D structure visualization representing each motif pattern. (A) Wild-type KPC-2 and its mutational variants. (B) Wild-type KPC-3 and its mutational variants

KPC-81 possesses an undiscovered Ω-loop motif because of a deletion of isoleucine at position 173 (del_I173) within its Ω-loop. This specific deletion is believed to increase the binding of CAZ, suggesting a conformational shift that might facilitate improved interaction or hydrolysis of CAZ by the enzyme, but when KPC-81 was cloned into *Escherichia coli* TOP10, it maintained susceptibility to carbapenems (Sanz et al., 2024). In KPC-154, there is amino acid duplication (RAPNKDDKYS) in positions 263–273, which corresponds to the 270 loop. This conformational change gives KPC-154 higher minimum inhibitory concentration (MIC) for several β-lactams, compared to the isogenic KPC-31 carrying strain (Arcari et al., 2023). KPC-135 is characterized by seven amino acid insertion (Ser-Ala-Asn-Asp-Ala-Ser-Leu) into the 266-275 loop region. This insertion is analogous to, but different from the 15-amino acid duplication seen in KPC-44. The seven-amino-acid insertion directly contributes to CAZ-AVI resistance by altering the active site conformation and reducing AVI inhibitory effect. According to Shi et al. (2024) study, it does not explicitly state whether KPC-135 has a trade-off resulting in restored carbapenem susceptibility. However, the presence of the insertion in the 266-275 loop suggests that it might have some impact on carbapenem hydrolysis.

KPC-201 originated from KPC-3 and shows a unique LDR amino acid deletion at positions 161-163. This deletion results in a more open active site, which is believed to be the reason for its resistance to CAZ-AVI. Although KPC-201 confers CAZ resistance, it notably regains susceptibility to carbapenems, unlike the wild-type which remains resistant to carbapenems (Hu et al., 2024). KPC-9 differs from KPC-3 as the wild-type due to a single amino acid substitution from valine to alanine at position 293 (Val239Ala). This specific mutation alters the enzymatic behavior. Compared to KPC-3, KPC-9 exhibits reduced resistance to carbapenem antibiotics like imipenem, ertapenem, and meropenem. Conversely, KPC-9 shows an increased ability to resist CAZ, with kinetic studies indicating KPC-9 enzyme hydrolyzes CAZ more efficiently than KPC-3 (Hidalgo-Grass et al., 2012).

Based on the current search results for KPC-257, KPC-258 and KPC-117, there were no dedicated published research papers that specifically discuss the molecular mechanisms, conformational changes, and direct comparisons of the KPC variant resistance profiles to KPC-2 or any other KPC variants in the same way as the other variants like KPC-44, KPC-109, KPC-115, KPC-73, KPC-135, or KPC-201. From the resistance profile comparison across different motif composition and conformational changes, even though most of the analyzed KPC mutant variants often share the clinical characteristic of exhibiting resistance to CAZ-AVI, they also accompanied by a trade-off leading to restored or maintained susceptibility to carbapenems. While enzymatic studies mainly show restored carbapenem susceptibility, in real-world clinical isolates, other resistance mechanisms like porin deficiencies, efflux pump overexpression can co-exist and might still lead to high carbapenem MIC.

3.5 Molecular docking analysis

KPC-2 has become the most widespread clinical allele and is commonly used as a reference because its substrate and inhibitor profiles have been extensively studied. KPC-3 is a single variant that is structurally very similar to KPC-2 but exhibits several phenotypic differences toward carbapenems because of a single amino acid change at position 272 from histidine to tyrosine in the KPC-3 variant and its derivatives. Eleven KPC variants from the KPC-2 and KPC-3 clusters showing different motif compositions were further analyzed by molecular docking against several antibiotics and inhibitors commonly used in clinical settings to treat *K. pneumoniae* infections such as CAZ, AVI, IPM, MEM, and ATM.

Molecular docking results show that in the KPC-2 cluster (Table 3), many variants such as KPC-44, KPC-117, KPC-133, KPC-135, and KPC-258 shows binding affinity values ranged from approximately -8.1 to -8.8 with CAZ. These values are more negative compared to IPM or MEM which ranged from -6.6 to -7.9. Meanwhile, several variants in the KPC-2 cluster show binding affinities with AVI between -7.1 and -8.2. Docking results of several KPC-3 cluster variants (Table 4) with CAZ also showed more negative binding affinities of around -8.0 to -8.1 although some variants such as KPC-66 exhibited changes.

The binding affinity (docking score) of several KPC variants in cluster 2 with CAZ being more negative indicates a relatively stronger predicted interaction at the target site. In the KPC cluster 3 variants, the stronger binding of CAZ compared to IPM/MEM suggests a similar phenotypic pattern associated with increased CAZ hydrolysis capability or altered substrate selectivity. Based on this, CAZ appears to be a more efficient inhibitor of KPC and has the potential to serve as an antibiotic candidate against mutant KPC variants through its hydrolytic orientation and serine-catalytic inactivation mechanism. Docking results (Table 3) consistently show that KPC variants with insertions or deletions in the Ω-loop tend to favor CAZ hydrolysis and may trigger CAZ-AVI resistance if AVI loses its optimal affinity or inhibitory interaction. Previous studies reported that insertions or deletions in the Ω-loop or mutations at specific positions can increase resistance to CAZ-AVI or reduce AVI binding, although the specific effect depends on the exact mutation and plasmid/porin context, which can decrease the effectiveness of AVI (Sun et al., 2024). Meanwhile, the docking patterns of several KPC cluster 3 variants show higher affinity of CAZ compared to IPM/MEM, suggesting that CAZ hydrolysis is more favorable (Wei et al., 2025).

Visualization of the molecular docking results was performed on KPC-2, KPC-3, KPC-135, and KPC-201 variants with the inhibitor (antibiotic) CAZ, based on their highest binding affinity values compared to other variants. KPC-135 is a derivative cluster of KPC-2, while KPC-201 is a derivative cluster of KPC-3. The literature indicates that a stronger binding affinity predicted by docking correlates with increased catalytic activity, as observed in this study for CAZ. Consequently, the MIC against CAZ tends to be high. Sun et al. (2024) explained that a high MIC, particularly associated with elevated catalytic efficiency of CAZ, can reduce the overall efficiency against carbapenems. Therefore, these findings are consistent with the docking results, which demonstrate that CAZ exhibits stronger binding compared to IPM or MEM in several KPC variants

Based on the comparison between the binding affinity values obtained in this study and the MIC data reported by Wei et al. (2025), a positive correlation was observed between the binding strength of CAZ to the KPC enzyme and the level of antibiotic resistance. KPC variants with more negative binding affinity values, such as KPC-133 (-8.7 kcal/mol) and KPC-135 (-8.8 kcal/mol), tended to exhibit higher MIC values (≥ 32 mg/L) against CAZ, indicating increased resistance. This suggests that the stronger the interaction of CAZ with the active site of the β-lactamase enzyme, the higher the hydrolytic efficiency, leading to reduced antibacterial activity of CAZ. In contrast, variants such as KPC-81 (-7.8 kcal/mol) and KPC-257 (-7.8 kcal/mol), which displayed weaker binding affinities, were predicted to have lower MIC values, reflecting more limited hydrolytic activity against CAZ. These findings align with the report by Sun et al. (2024), which stated that stronger binding within the β-lactamase–CAZ complex contributes to enhanced catalytic efficiency toward β-lactam antibiotics. Therefore, the molecular docking results in this study support the phenotypic data reported by Wei et al. (2025), showing that KPC-2 derivatives such as KPC-135 contribute to increased resistance through optimized interactions within the active regions (the 270-loop and Ω-loop). Overall, these results confirm that subtle structural modifications within the active-site residues of KPC can lead to significant differences in binding strength and hydrolytic efficiency, directly influencing MIC values and clinical resistance to CAZ.

Table 3. Binding affinity of different KPC variants in KPC-2 cluster

Reference	Change Introduced	KPC Variant	Binding Affinity (kcal/mol)				
			CAZ	AVI	IPM	MEM	ATM
Wang et al. 2015	-	KPC-2	-8.1	-7.2	-6.9	-7.8	-7.3
Sun et al., 2024	15 amino acid duplication in one of the active-site loops (270-loop)	KPC-44	-8.5	-7.1	-7.2	-6.7	-7.8
Hobson et al., 2022	Insertion of 265RAPNKDDN	KPC-58	-8.1	-6.4	-7.2	-7.9	-7.2
Sanz et al., 2024	Deletion of the I173 within the Ω-loop	KPC-81	-7.8	-7.1	-7.4	-7.8	-7.3
-	Single amino acid change at L6I, and insertion of 3RCP and 10F	KPC-117	-8.2	-7.1	-7.1	-7.9	-7.5
-	Single amino acid change at D182G and the insertion of 273DDKHSEAVYTRAPNK	KPC-133	-8.7	-8.2	-7.6	-7.9	-7.7
Shi et al., 2024	Deletion of the E168 and L169, and a 15-amino acid tandem repeat between V262 and A276	KPC-135	-8.8	-8.2	-7.5	-7.4	-7.2
-	Deletion of the E171 and L172, and insertion of 280VYTRAPNK	KPC-257	-7.8	-7.2	-6.9	-7.9	-7.3
-	Single amino acid change at L165H and D166G, and deletion of R167, W168, E169, L170, E171, L172, N173, S174, A175, I176, P177, G178, and D179	KPC-258	-8.1	-7	-6.6	-7.2	-7.5

Table 4. Binding affinity of different KPC variants in KPC-3 cluster

Reference	Change Introduced	KPC Variant	Binding Affinity (kcal/mol)				
			CAZ	AVI	IPM	MEM	ATM
Migliorini et al., 2021	Single amino acid change at H272Y	KPC-3	-8.1	-6.5	-7.0	-7.9	-7.7
Hidalgo-Grass et al., 2012	Single amino acid substitution at V239A	KPC-9	-8.0	-7.2	-7.3	-7.7	-7.2
Hobson et al., 2022	Deletion of the E168 and L169	KPC-66	-7.3	-7.2	-6.8	-8.1	-6.8
Hu et al., 2024	Deletion of the amino acids LDR at positions 161–163	KPC-201	-8.1	-6.3	-7.3	-6.0	-7.6

Molecular docking analysis demonstrated that CAZ is bound within the catalytic pocket of KPC variants (KPC-2, KPC-135, KPC-3, and KPC-201), yet with distinct residue interaction profiles (Figure 7). In KPC-2, CAZ engages a dense hydrogen-bond network with Ser69, Asn131, Glu165, Lys233, and Thr234, indicating stable binding within the conserved β-lactamase catalytic groove. The KPC-135 complex exhibits a rearranged binding pattern, dominated by hydrogen bonds with Ser69, Ser129, Thr234, Thr236, alongside π-interactions with Trp104. In KPC-3, the ligand maintained interactions with Ser69, Asn131, Thr234, Thr236, Cys237, and Tyr272, supported by hydrophobic stabilization from Trp104. Meanwhile, KPC-201 displayed a more shifted network, with hydrogen bonds involving Ser69, Asn131, Asn169, Glu165, Leu166, Thr234, and Thr236, as well as π-sulfur and π-alkyl interactions contributed by Trp104 and Tyr272. These variations suggest structural remodeling across the four enzymes, particularly within the Ω-loop and surrounding residues that shape the catalytic cleft.

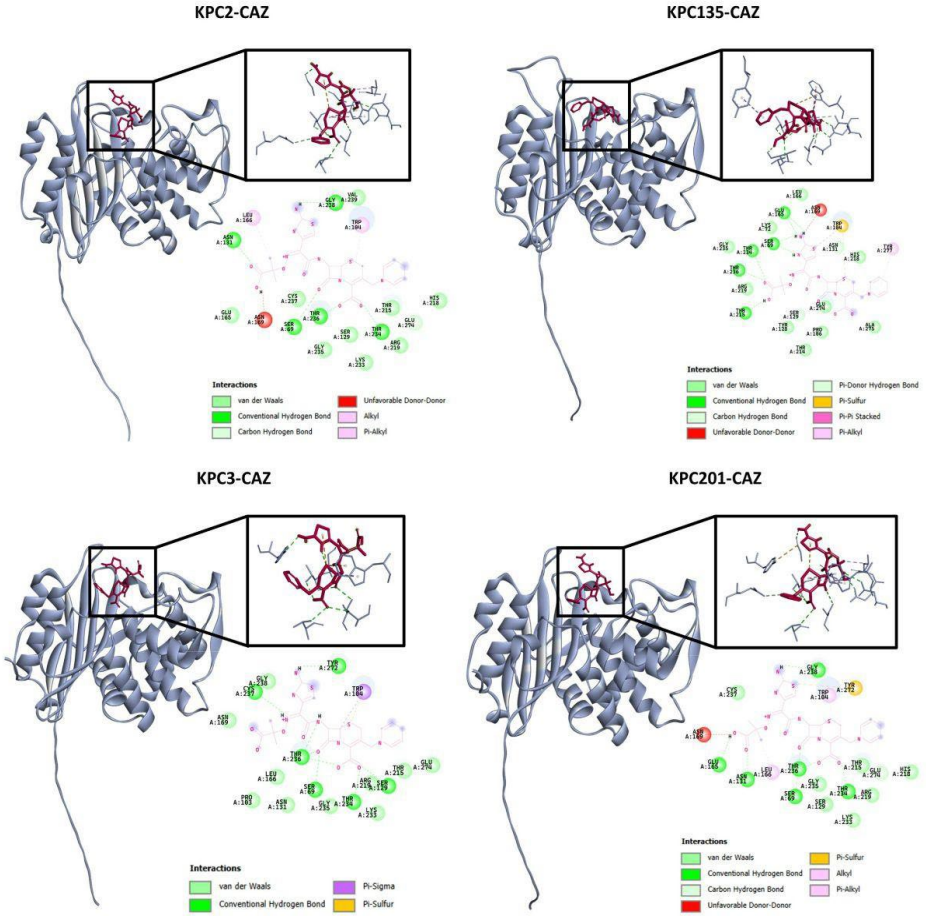

Figure 7. Molecular docking and interaction between KPC-2, KPC-135, KPC-3, and KPC-201 with ceftazidime (CAZ)

The observed differences in hydrogen-bonding patterns and hydrophobic interactions reflect how amino acid substitutions modulate the geometry and dynamics of the KPC active site. The strong interaction of CAZ with catalytic residues Ser69 (Ser70), Asn132, and Glu166 in KPC-2 supports efficient substrate hydrolysis typical of class A β-lactamases (Mehta et al., 2021). In contrast, KPC-135 displays a marked reorganization of its active-site architecture due to the substitution at position 234 and rearrangement of the Ω-loop, as previously reported by Shi et al. (2024). These structural changes enlarge the catalytic cavity and weaken key hydrogen bonds with Asn132 and Thr235, thereby improving accommodation of bulky substrates like CAZ but reducing AVI affinity. Similarly, KPC-3 retains the canonical catalytic orientation yet shows increased Ω-loop flexibility that may enhance ligand accommodation. KPC-201, on the other hand, exhibits a broader but less stable pocket, consistent with an adaptive compromise between catalytic efficiency and inhibitor escape. Collectively, these findings indicate that while all variants preserve the core catalytic serine, their evolutionary trajectory involves local rearrangements that balance β-lactam hydrolysis and resistance optimization.

4. Conclusions

Based on the results of the analysis of physicochemical properties, genetic variations between mutant and wild-type KPC strains mainly occur in the isoelectric point parameters, instability index, high aliphatic index, and GRAVY. The results of the protein motifs analysis show 11 different motif patterns from the wild-type. Conservative motifs are maintained in most variants, indicating the same evolutionary origin, with KPC-2 as the main ancestor and KPC-3 as the early mutant. Structural conformational changes are dominated by changes in the active loop structure such as Ω-loop, 240-loop, and 270-loop, in which 11 different motif patterns from the wild-type were found. Different motif patterns and mutations in the loop area result in conformational changes such as hinge motion, rearrangement, and fold switch, which have the potential to increase resistance to antibiotics. Mutations in KPC variants tend to accumulate in structural elements that affect catalytic function, such as the active loop, while the core protein framework is maintained. Variants with complex motif patterns and significant structural changes such as KPC-9, KPC-117, KPC-135, KPC-201, and KPC-258 can be considered the most aberrant mutants, while variants within Haplotype 1 such as KPC-6, KPC-8, and other mutant variants that are in the same haplotype, are the closest to the wild-type, KPC-2 and KPC-3. Based on the molecular docking results, CAZ was identified as the strongest inhibitor against KPC-mediated infections in several variants.

5. Acknowledgements

The authors wish to express their profound appreciation to Dr. Dewi Santosaningsih, M.Kes, Sp.MK, Ph.D, from Department of Clinical Microbiology, Faculty of Medicine, Brawijaya University, for her invaluable insights and expertise regarding antibiotic resistance, which significantly contributed to the preparation of this article. Furthermore, the successful completion of this research was facilitated by the access to the computational laboratory at the Faculty of Mathematics and Natural Sciences, Brawijaya University, Malang.

6. Authors' Contributions

Muhammad Yusuf Airlangga: Conceptualization, performed the bioinformatics analysis, and writing - original drafting; Riffatih Syah Maharani, Amanda Rossiana Putri & Marita Tasya Andriasari: Performed the bioinformatics analysis, and writing -original drafting; Balqis Salsabillah Shifa Fithryyh Cuhada: Performed the bioinformatics analysis, and writing - original drafting; Nuraini Rosyadah: writing - review and editing; Fatchiyah Fatchiyah, Eko Suyanto, & Turhadi Turhadi: Supervision and writing - review and editing.

7. Conflicts of Interest

The authors declare that they have no conflicts of interest.

References

Acman, M., Wang, R., van Dorp, L., Shaw, L. P., Wang, Q., Luhmann, N., Yin, Y., Sun, S., Chen, H., Wang, H., & Balloux, F. (2022). Role of mobile genetic elements in the global dissemination of the carbapenem resistance gene *bla*$_{NDM}$. *Nature Communications, 13*, Article 1131. https://doi.org/10.1038/s41467-022-28819-2

Arcari, G., Cecilia, F., Oliva, A., Polani, R., Raponi, G., Sacco, F., Francesco, A. D., Pugliese, F., & Carattoli, A. (2023). Genotypic evolution of *Klebsiella pneumoniae* sequence type 512 during ceftazidime/avibactam, meropenem/vaborbactam, and cefiderocol treatment, Italy. *Emerging Infectious Diseases*, *29*(11), 2266-2274. https://doi.org/10.3201/eid2911.230921

Bailey, T. L., Johnson, J., Grant, C. E., & Noble, W. S. (2015). The MEME suite. *Nucleic Acids Research, 43*(1), 39-49. https://doi.org/10.1093/nar/gkv416

Bongiorno, D., Bivona, D. A., Cicino, C., Trecarichi, E. M., Russo, A., Marascio, N., Mezzatesta, M. L., Musso, N., Privitera, G. F., Quirino, A., Scarlata, G. G. M., Matera, G., Torti, C., & Stefani, S. (2023). Omic insights into various ceftazidime-avibactam-resistant *Klebsiella pneumoniae* isolates from two southern Italian regions. *Frontiers in Cellular and Infection Microbiology, 12*, Article 1010979. https://doi.org/10.3389/fcimb.2022.1010979

Brandt, C., Viehweger, A., Sigh, A., Pletz, M. W., Wibberg, D., Kalinowski, J., Lurch, S., Müller, B., & Makarewicz, O. (2019). Assessing genetic diversity and similarity of 453 KPC carrying plasmids. *Scientific Reports*, *9*, Article 11223. https://doi.org/10.1038/s41598-019-47758-5

Bryant, P. & Noé, F. (2024). Structure prediction of alternative protein conformations. *Nature Communications*, *15*, Article 7328. https://doi.org/10.1038/s41467-024-51507-2

Cai, M., Song, K., Wang, R., Wang, S., Chen, H., & Wang, H. (2024). Tracking intra-species and inter-genus transmission of KPC through global plasmids mining. *Cell Reports*, *43*(6), Article 114351. https://doi.org/10.1016/j.celrep.2024.114351

Chen, L., Ai, W., Zhou, Y., Wu, C., Guo, Y., Wu, X., Wang, B., Rao, L., Xu, Y., Zhang, J., Cheng, L., & Yu, F. (2022). Outbreak of *IncX8* plasmid–mediated KPC-3–producing *Enterobacterales* infection, China. *Emerging Infectious Diseases, 28*(7), 1421-1430. https://doi.org/10.3201/eid2807.212181

Ding, L., Shen, S., Chen, J., Tian, Z., Shi, Q., Han, R., Yan, G., & Hu, F. (2023). *Klebsiella pneumoniae* carbapenemase variants: the new threat to global public health. *Antimicrobial Chemotherapy, 36*(4), 1-26. https://doi.org/10.1128/cmr.00008-23

Falagas, M. E., Asimotou, C.-M., Zidrou, M., Kontogiannis, D. S., & Filippou, C. 2025. Global epidemiology and antimicrobial resistance of *Klebsiella pneumoniae* carbapenemase

(KPC)-producing gram-negative clinical isolates: a review. *Microorganisms, 13*(7), Article 1697. https://doi.org/10.3390/microorganisms13071697

Fontana, C., Favaro, M., Campogiani, L., Malagnino, V., Minelli, S., Bossa, M. C., Altieri, A., Andreoni, M., & Sarmati, L. (2021). Ceftazidime/avibactam-resistant *Klebsiella pneumoniae* subsp. *pneumoniae* isolates in a tertiary Italian hospital: identification of a new mutation of the carbapenemase type 3 (KPC-3) gene conferring ceftazidime/avibactam resistance. *Microorganisms, 9*(11), Article 2356. https://doi.org/10.3390/microorganisms9112356

Garsevanyan, S., & Barlow, M. (2024). The *Klebsiella pneumoniae* carbapenemase (KPC) β-Lactamasehas evolved in response to ceftazidime avibactam. *Antibiotics, 13*(1), Article 40. https://doi.org/10.3390/antibiotics13010040

Giddins, M. J., Macesic, N., Annavajhala, M. K., Stump, S., Khan, S., McConville, T. H., Mehta, M., Gomez-Simmond, A., & Uhlemann, A.-C. (2018). Successive emergence of ceftazidime-avibactam resistance through distinct genomic adaptations in *bla*$_{KPC-2}$-harboring *Klebsiella pneumoniae* sequence type 307 isolates. *Antimicrobial Agents and Chemotherapy*, *62*, 2101-2117. https://doi.org/10.1128/aac.02101-17

Gouripur, G. C., Kaliwal, R. B., & Kaliwal, B. B. (2016). In silico characterization of beta-galactosidase using computational tools. *Journal of Bioinformatics and Sequence Analysis*, *8*(1), 1-11. https://doi.org/10.5897/JBSA2015.0101

Guo, L., Wang, L., Zhao, Q., Ye, L., Ye, K., Ma, Y., Shen, D., & Yang, J. (2022). Genomic analysis of KPC-2-producing *Klebsiella pneumoniae* ST11 isolates at the respiratory department of tertiary care hospital in Beijing, China. *Frontier in Microbiology*, *13*, Article 929826. https://doi.org/10.3389/fmicb.2022.929826

Guruprasad, L. (2019). Protein structure. *Resonance, 24*(3), 327-338. https://doi.org/10.1007/s12045-019-0783-7

Ha, J.-H. & Loh, S. N. (2012). Protein conformational switches: From nature to design. *Chemistry - A European Journal*, *18*(26), 7984-7999. https://doi.org/10.1002/chem.201200348

Hidalgo-Grass, C., Warburg, G., Temper, V., Benenson, S., Moses, A. E., Block, C., & Strahilevitz, J. (2012). KPC-9, a novel carbapenemase from clinical specimens in Israel. *Antimicrobial Agents and Chemotherapy*, *56*(11), 6057-6059. https://doi.org/10.1128/aac.01156-12

Hobson, C. A., Pierrat, G., Tenaillon, O., Bonacorsi, S., Bercot, B., Jaouen, E., Jacquier, H., & Birgy, A. (2022). *Klebsiella pneumoniae* carbapenemase variants resistant to ceftazidime-avibactam: an evolutionary overview. *Antimicrobial Agents and Chemotherapy, 66*(9), Article e00447-22. https://doi.org/10.1128/aac.00447-22

Hu, Y., Shen, W., Lin, D., Wu, Y., Zhang, Y., Zhau, H., Zhang, R. (2024). KPC variants conferring resistance to ceftazidime-avibactam in *Pseudomonas aeruginosa* strains. *Microbiological Research*, *289*, Article 127893. https://doi.org/10.1016/j.micres.2024.127893

Huang, X., Shen, S., Chang, F., Liu, X., Yue, J., Xie, N., Yin, L., Hu, F., & Xiao, D. (2023). Emergence of KPC-134, a KPC-2 variant associated with ceftazidime-avibactam resistance in a ST11 *Klebsiella pneumoniae* clinical strain. *Microbiology Spectrum, 11*(5), 723-725. https://doi.org/10.1128/spectrum.00725-23

Lau, A. M., Bordin, N., Kandathil, S. M., Sillitoe, I., Waman, V. P., Wells, J., Orengo, C. A., & Jones, D. T. (2024). Exploring structural diversity across the protein universe with The Encyclopedia of Domains. *Science*, *386*(6721), Article edq4946. https://doi.org/10.1126/science.adq4946

Ling, Z.-N., Jiang, Y.-F., Ru, J.-N., Lu, J.-H., Ding, B., & Wu, J. (2023). Amino acid metabolism in health and disease. *Signal Transduction and Targeted Therapy*, *8*(1), Article 345. https://doi.org/10.1038/s41392-023-01569-3

Mehta, S. C., Furey, I. M., Pemberton, O. A., Boragine, D. M., Chen, Y., & Palzkill, T. (2021). KPC-2 β-lactamase enables carbapenem antibiotic resistance through fast deacylation of the covalent intermediate. *Journal of Biological Chemistry*, *296*, Article 100155. https://doi.org/10.1074/jbc.RA120.015050

Migliorini, L. B., de Sales, R. O., Koga, P. C. M., Doi, A. M., Poehlein, A., Toniolo, A. R., Menezes, F., Martino, M., Gales, A. C., Bruggemann, H., & P. Saverino. (2021). Prevalence of *bla*$_{KPC-2}$, *bla*$_{KPC-3}$ and *bla*$_{KPC-30}$—carrying plasmids in *Klebsiella pneumoniae* isolated in a Brazilian hospital. *Pathogens, 10*(3), Article 332. https://doi.org/10.3390/pathogens10030332

Mohanta, T. K., Kamran, M. S., Omar, M., Anwar, W., & Choi, G. S. (2022). PlantMW*p*I DB: a database for the molecular weight and isoelectric points of the plant proteomes. *Scientific Reports, 12*(1), Article 7421. https://doi.org/10.1038/s41598-022-11077-z

Moraes Filho, R. M., Rossiter, J. G., Cavalcanti Junior, E. A., & Martins, L. S. S. (2017). *In silico* comparative analysis of legume lectins. *Journal of Genetics and Genomes, 1*(1), 1-11.

Nicola, F., Cejas, D., Gonzālez-Espinosa, F., Relloso, S., Herrera, F., Bonvehi, P., Smayevsky, J., Figueroa-Espinosa, R., Gutkind, G., & Radice, M. (2022). Outbreak of *Klebsiella pneumoniae* ST11 resistant to ceftazidime-avibactam producing KPC-31 and the novel variant KPC-115 during COVID-19 pandemic in Argentina. *Microbiology Spectrum*, *10*(6), Article e03733-22. https://doi.org/10.1128/spectrum.03733-22

Ourghanlian, C., Soroka, D., & Arthur, M. (2017). Inhibition by avibactam and clavulanate of the β-lactamases KPC-2 and CTX-M-15 harboring the substitution N132G in the conserved SDN motif. *Antimicrobial Agents and Chemotherapy*, *61*(3), Article e02510-16. https://doi.org/10.1128/AAC.02510-16

Partridge, S. R., Kwong, S. M., Firth, N., & Jensen, S. O. (2018). Mobile genetic elements associated with antimicrobial resistance. *Clinical Microbiology Reviews, 31*(4), 8-17. https://doi.org/10.1128/CMR.00088-17

Permana, S., Nurzaidah, L., Widodo, E., Anita, K. W., Nugraheni, R. W., Kawamoto, Y., Endrawati, H., & Endharti, A. T. (2024). Anticancer activity of *Hedyotis corymbosa* nanoliposomes targeting estrogen receptor-alpha in breast cancer cells: *In silico* and *in vitro* studies. *Journal of Pharmacy and Pharmacognosy Research*, *12*(12), 303-322. https://doi.org/10.56499/jppres23.1783_12.2.303

Pilato, V. D., Codda, G., Niccolai, C., Willison, E., Wong, J. L. C., Coppo, E., Frankel, G., Marchese, A., Rossolini, G. M. (2024). Functional features of KPC-109, a novel 270-loop KPC-3 mutant mediating resistance to avibactam-based β-lactamase inhibitor combinations and cefiderocol. *International Journal of Antimicrobial Agents*, *63*(1), Article 107030. https://doi.org/10.1016/j.ijantimicag.2023.107030

Qiao, S., Xin, S., Zhu, Y., Zhao, F., Wu, H., Zhang, J., Yao, B., Yu, Y., Fu, Y., Jiang, Y., Xie, X., & Zhang, J. (2024). A large-scale surveillance revealed that KPC variants mediated ceftazidime-avibactam resistance in clinically isolated *Klebsiella pneumoniae. Microbiology Spectrum, 12*(8), Article e0025824. https://doi.org/10.1128/spectrum.00258-24

Rachmi, E., Purnomo, B. B., Endharti, A. T., & Fitri, L. E. (2020). In silico prediction of anti-apoptotic BCL-2 proteins modulation by Afzelin in MDA-MB-231 breast cancer cell. *Research Journal of Pharmacy and Technology*, *13*(2), 905-910. https://doi.org/10.56499/jppres23.1783_12.2.303

Rada, A. M., Cadena, E. D. L., Agudelo, C., Capataz, C., Orozco, N., Pallares, C., Dinh, A. Q., Panesso, D., Ríos, R., Diaz, L., Correa, A., Hanson, B. M., Villegas, M. V., Arias, C. A., & Restrepo, E. (2020). Dynamics of *bla*$_{KPC-2}$ dissemination from non-CG258 *Klebsiella pneumoniae* to other *Enterobacterales* via IncN plasmids in an area of high

endemicity. *Antimicrobial Agents and Chemotherapy*, *64*(12), Article e01743-20. https://doi.org/e01743-20. https://doi.org/10.1128/AAC.01743-20

Rocha, J., Henriques, I., Gomila, M., & Manaia, C. M. (2022). Common and distinctive genomic features of *Klebsiella pneumoniae* thriving in the natural environment or in clinical settings. *Scientific Reports*, *12*(1), Article 10441. https://doi.org/10.1038/s41598-022-14547-6

Rozas, J., Ferrer-Mata, A., Sánchez-DelBarrio, J. C., Guirao-Rico, S., Librado, P., Ramos-Onsins, S. E., & Sánchez-Gracia, A. (2017). DnaSP 6: DNA sequence polymorphism analysis of large data sets. *Molecular Biology and Evolution, 34*(12), 3299-3302. https://doi.org/10.1093/molbev/msx248

Rubalakshmi, G., Vidya, M., Nirubama, K., Prabhakaran, S., & Mehanathan, A. (2020). Structural evaluation and insilico study of proteins of asterias rubens- “starfish as new source to marine proteins”. *Kongunadu Research Journal, 7*(1), 19-27. https://doi.org/10.26524/krj.2020.4

Sanz, M. B., Pasteran, F., de Mendieta, J. M., Brunetti, F., Albornoz, E., Rapoport, M., Lucero, C., Errecalde, L., Nuñez, M. R., Monge, R., Pennini, M., Power, P., Corso, A., & Gomez, S. A. (2024). KPC-2 allelic variants in *Klebsiella pneumoniae* isolates resistant to ceftazidime-avibactam from Argentina: bla_{KPC-80}, bla_{KPC-81}, bla_{KPC-96} and bla_{KPC-97}. *Microbiology Spectrum*, *12*(3), 4111-4123. https://doi.org/10.1128/spectrum.04111-23

Satapoomin, N., Dulyayangkul, P., & Avison, M. B. (2022). *Klebsiella pneumoniae* mutants resistant to ceftazidime-avibactam plus aztreonam, imipenem-relebactam, meropenem-vaborbactam, and cefepime-taniborbactam. *Antimicrobial Agents and Chemotherapy, 66*(4), Article e02179-21. https://doi.org/10.1128/aac.02179-21

Shi, Q., Han, R., Guo, Y., Yang, Y., Wu, S., Ding, L., Zhang, R., Yin, D., & Hu, F. (2022). Multiple novel ceftazidime-avibactam-resistant variants of *bla*KPC-2-positive *Klebsiella pneumoniae* in two patients. *Microbiology Spectrum, 10*(1), 1714-1721. https://doi.org/10.1128/spectrum.01714-21

Shi, Q., Shen, S., Tang, C., Ding, L., Guo, Y., Yang, Y., Wu, S., Han, R., Yin, D., & Hu, F. (2024). Molecular mechanisms responsible KPC-135-mediated resistance to ceftazidime-avibactam in ST11-K47 hypervirulent *Klebsiella pneumoniae*. *Emerging Microbes and Infections*, *13*(1), Article 2361007. https://doi.org/10.1080/22221751.2024.2361007

Shields, R. K., Chen, L., Cheng, S., Chavda, K. D., Press, E. G., Snyder, A., Pandey, R., Doi, Y., Kreiswirth, B. N., Nguyen, M. H., & Clancy, C. J. (2017). Emergence of ceftazidime-avibactam resistance due to plasmid-borne bla_{KPC-3} mutations during treatment of carbapenem-resistant *Klebsiella pneumoniae* infections. *Antimicrobial Agents and Chemotherapy, 61*(3), Article e2097-16. https://doi.org/10.1128/aac.02097-16

Sugita, K., Aoki, K., Komori, K., Nagasawa, T., Ishii, Y., Iwata, S., & Tateda, K. (2021). Molecular analysis of bla_{KPC-2}-harboring plasmids: Tn*4401a* interplasmid transposition and Tn*4401a*-carrying ColRNAI plasmid mobilization from *Klebsiella pneumoniae* to *Citrobacter europaeus* and *Morganella morganii* in a single patient. *mSphere*, *6*(6), Article e00850-21. https://doi.org/10.1128/mSphere.00850-21

Sun, L., Li, H., Wang, Q., Liu, Y., & Cao, B. (2021). Increased gene expression and copy number of mutated bla_{KPC} lead to high-level ceftazidime/avibactam resistance in *Klebsiella pneumoniae. BMC Microbiology, 21*, Article 230. https://doi.org/10.1186/s12866-021-02293-0

Sun, Z., H. Lin, H., Hu, L., Neetu, N., Sankaran, B., Wang, J., Prasad, B. V. V., & Palzkill, T. (2024). *Klebsiella pneumoniae* carbapenemase variant 44 acquires ceftazidime-avibactam resistance by altering the conformation of active-site loops. *Journal of Biological Chemistry*, *300*(1), Article 105493. https://doi.org/10.1016/j.jbc.2023.105493

Tooke, C. L., Hinchliffe, P., Beer, M., Zinovjev, K., Colenso, C. K., Schofield, C. J., Mulholland, A. J., & Spencer, J. (2023). Tautomer-Specific Deacylation and Ω-Loop Flexibility Explain the Carbapenem-Hydrolyzing Broad-Spectrum Activity of the KPC-

2 β-Lactamase. *Jounal of the American Chemical Society*, *145*(13), 7166-7180. https://doi.org/10.1021/jacs.2c12123

Tsai, C.-L., Kubota, K., Pham, H.-T., & Yeh, W.-B. (2021). Ancestral haplotype retention and population expansion determine the complicated population genetic structure of the hilly lineage of *Neolucanus swinhoei* complex (Coleoptera, Lucanidae) on the subtropical Taiwan island. *Insects, 12*(3), Article 227. https://doi.org/10.3390/insects12030227

Wang, D., Chen, J., Yang, L., Mou, Y., & Yang, Y. (2014). Phenotypic and enzymatic comparative analysis of the KPC variants, KPC-2 and its recently discovered variant KPC-15. *PLOS One, 9*(10). Article e111491. https://doi.org/10.1371/journal.pone.0111491

Wang, Y., Sholeh, M., Yang, L., Shakourzadeh, M. Z., Beig, M., & Azizian, K. (2025). Global trends of ceftazidime–avibactam resistance in gram-negative bacteria: systematic review and meta-analysis. *Antimicrobial Resistance and Infection Control*, *14*, Article 10. https://doi.org/10.1186/s13756-025-01518-5

Wargasetia, T. L., Ratnawati, H., Widodo, N., & Widyananda, M. H. (2021). Bioinformatics study of sea cucumber peptides as antibreast cancer through inhibiting the activity of overexpressed protein (EGFR, PI3K, AKT1, and CDK4). *Cancer Informatics*, *20*, 1-11. https://doi.org/10.1177/11769351211031864

Wei, J., Huang, J., Zou, C., Shen, S., Kreiswirth, B. N., Huang, A., & Niu, S. (2025). Diverse evolutionary trajectories of *Klebsiella pneumoniae* carbapenemase: unraveling the impact of amino acid substitutions on β-lactam susceptibility and the role of avibactam in driving resistance. *mSystems, 10*(4), 125-184. https://doi.org/10.1128/msystems.00184-25

Widyananda, M. H., Pratama, S. K., Ansori, A. N. M., Antonius, Y., Kharisma, V. D., Murtadlo, A. A. A., Jakhmota, V., Rebezov, M., Khayrullin, M., Derkho, M., Ullah, E., Susilo, R. J. K., Hayaza, S., Nugraha, A. P., Proboningrat, A., Fadholly, A., Sibero, M. T., & Zainul, R. (2023). Quercetin as an anticancer candidate for glioblastoma multiforme by targeting AKT1, MMP9, ABCB1, and VEGFA: an in silico study. *Karbala International Journal of Modern Science*, *9*(3), Article 10. https://doi.org/10.33640/2405-609X.3312

Xie, Y., Zu, C., Yi-Han, S., Xiyue, S., Le-Le, W., Dong, W., Jianfeng, Z., Yiting, W., Gang, L., & Jin-Fu, X. (2025). Transposition of insertion sequence element from KPC plasmid enhances intracellular survival of *Klebsiella pneumoniae*. *eBiomedicine*, *120*, Article 105944. https://doi.org/10.1016/j.ebiom.2025.105944

Zhang, X., Xie, Y., Zhang, Y., Lei, T., Zhou, L., Yao, J., Liu, L., Liu, H., He, J., Yu, Y., Tu, Y., & Li, X. (2024). Evolution of ceftazidime–avibactam resistance driven by mutations in double-copy bla_{KPC-2} to $bla_{KPC-189}$ during treatment of ST11 carbapenem-resistant *Klebsiella pneumoniae. Bacteriology, 9*(10), Article e00722-24 https://doi.org/10.1128/msystems.00722-24

Zhang, Y., Li, Z., Shi, H., Lei, Z., Pu, D., Liu, Q., Zhang, F., Zhao, J., Liu, X., Lu, B., & Cao, B. (2025). High-level ceftazidime-avibactam resistance by in-host evolution of bla_{KPC} genes: Emergence of a novel $bla_{KPC-102}$ variant and increase of bla_{KPC-33} copy number in *Klebsiella pneumoniae* strains from a lung transplantation recipient. *International Journal of Antimicrobial Agents, 66*(2), Article 107521. https://doi.org/10.1016/j.ijantimicag.2025.107521